Codimension-three bifurcations: Explanation of the complex one-, two-, and three-dimensional bifurcation structures in nonsmooth maps

Viktor Avrutin and Michael Schanz
IPVS, University of Stuttgart, Universitätstrasse 38, 70569 Stuttgart, Germany

Soumitro Banerjee
Department of Electrical Engineering, Indian Institute of Technology, Kharagpur-721302, India
(Received 7 August 2006; revised manuscript received 26 January 2007; published 8 June 2007)

Many physical and engineering systems exhibit cascades of periodic attractors arranged in period increment and period adding sequences as a parameter is varied. Such systems have been found to yield piecewise smooth maps, and in some cases the obtained map is discontinuous. By investigating the normal form of such maps, we have detected a type of codimension-three bifurcation which serves as the organizing center of periodic and aperiodic dynamics in the parameter space. The results will help in understanding the occurrence and structure of such cascades observed in many nonsmooth systems in science and engineering.

DOI: 10.1103/PhysRevE.75.066205 PACS number(s): 05.45.Ac

I. INTRODUCTION

In the investigations on practical dynamical systems as diverse as biological autocatalytic processes, optogalvanic circuits, impact oscillators, electronic switching circuits, and neural relaxation oscillators, a few typical bifurcation scenarios have been reported [1]. These are pure period increment, period increment with coexistence of attractors, and period adding scenarios, as illustrated in Fig. 1. In all three cases, there exists a sequence of periodic attractors, whose periods form an arithmetic series $p_n=p_0+n\Delta p$ with a starting period p_0 and an increment value Δp. Let μ_n be the parameter value at which the attractor with period p_n is created, and let $\bar{\mu}_n$ be the value at which it is destroyed. The common property of all three bifurcation scenarios mentioned above is that $\mu_n<\mu_{n+1}$ implies $\bar{\mu}_n<\bar{\mu}_{n+1}$. For the pure period increment scenario [Fig. 1(a)] the parameter value for the annihilation of one attractor is the same as that for the emergence of the next ($\bar{\mu}_n=\mu_{n+1}$), for the period increment with coexistence of attractors [Fig. 1(b)], the parameter ranges of the occurrence of attractors with incremental periods overlap ($\bar{\mu}_n>\mu_{n+1}$), and for the period adding scenario [Fig. 1(c)] there is a gap between the two ranges ($\bar{\mu}_n<\mu_{n+1}$).

In the last case we observe higher-periodic attractors in this gap, whose periods can be calculated based on p_n and p_{n+1} using the infinite adding scheme [2,3] as follows. Let Ψ be the symbolic sequence corresponding to the attractor with period p_n and Φ the one corresponding to the attractor with period p_{n+1}. Then, between periods p_n and p_{n+1}, there exists the period p_n+p_{n+1} (corresponding to the symbolic sequence $\Psi\Phi$), between periods p_n+p_{n+1} and p_{n+1} there exists the period p_n+2p_{n+1} (corresponding to the symbolic sequence $\Psi\Phi^2$), and so on. However, the gap between the two ranges ($\bar{\mu}_n<\mu_{n+1}$) does not necessarily lead to the period adding inclusions. For instance, in the gap a complete period-doubling scenario may occur, including ranges of chaotic behavior. In situations where high-periodic orbits are not stable, the dynamics in the gaps may be chaotic without any periodic inclusions. A typical example for this scenario is shown in Fig. 1(d).

The natural question is: How are these bifurcation scenarios organized? In probing this question, we note that most of the systems in which such bifurcation sequences have been observed yield nonsmooth maps on discrete modeling. Many of these systems (like the sigma-delta modulator, the Colpitts oscillator, and some switching electronic circuits) [4] have been shown to yield maps that are not only piecewise smooth, but also have a discontinuity at the border. Therefore, we investigate this problem using a general model [5] given by

$$x_{n+1}=f(x_n,a,b,\mu,l)=\begin{cases} ax_n+\mu & \text{if } x_n<0, \\ bx_n+\mu+l & \text{if } x_n>0. \end{cases} \quad (1)$$

In fact, the model (1) represents the piecewise linear approximation of general piecewise smooth maps in the neighborhood of the point of discontinuity, and all the bifurcation patterns mentioned above occur in this system. It has been shown [5] that in this system such characteristic bifurcation patterns are generated by repeated occurrence of border collision bifurcations.

In this paper we investigate the character of the parameter space of system (1). It is known that the parameter combinations for codimension-one bifurcations represent curves in two-dimensional (2D) parameter spaces and surfaces in three-dimensional (3D) parameter spaces. When dealing with 2D parameter spaces, the codimension-one bifurcation curves may intersect, whereby the intersection points represent codimension-two bifurcations. It has been shown that a special type of codimension-two bifurcation point may occur, where an infinite number of codimension-one curves intersect. This phenomenon has been named as codimension-two *big bang bifurcation* (BBB) [3,6]. In general, a codimension-N BBB point is defined as a point in an N-dimensional parameter space ($N\geq 2$), where an infinite number of codimension-$(N-1)$ bifurcation curves intersect.

By a suitable scaling, system (1) can be reduced to the three cases $l\in\{-1,0,1\}$. In the 3D parameter spaces of system (1) we find some generic bifurcation patterns for these three cases, which are responsible for the complex bifurcation structures observed in many practical systems. Thus, a framework for the explanation of these scenarios is provided

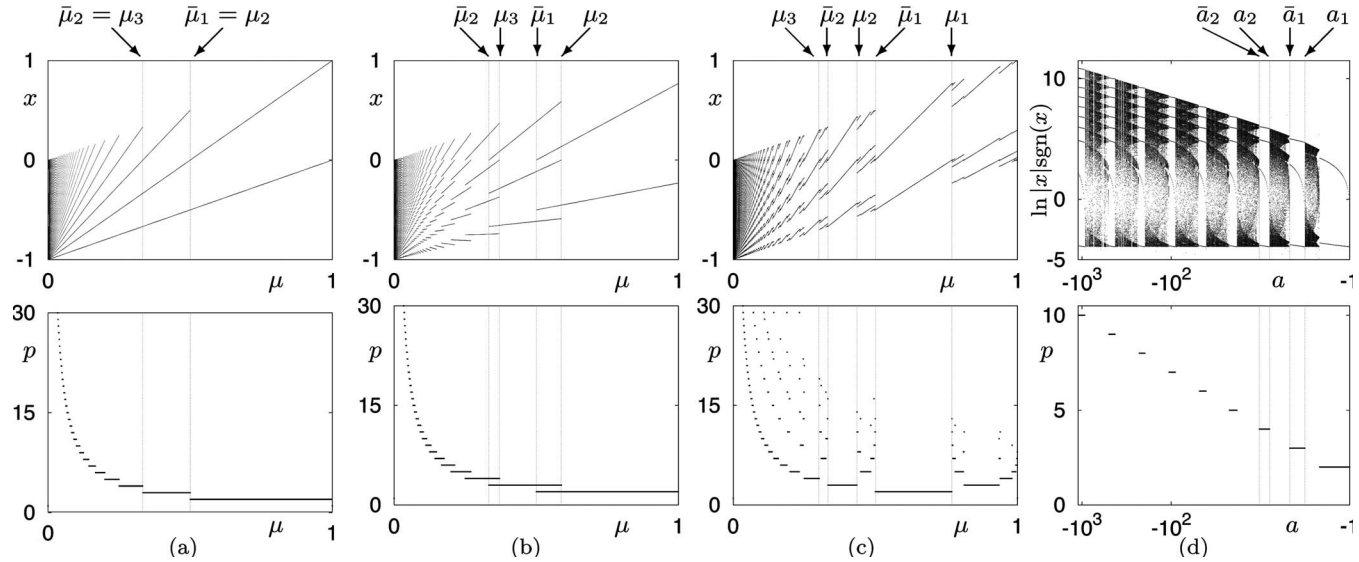

FIG. 1. Typical bifurcation scenarios observable in piecewise smooth maps under variation of one parameter: pure period increment (a), period increment with coexistence of attractors (b), period increment with period adding inclusions (c), and period increment with chaotic inclusions (d). Top row: one-parameter bifurcation diagrams; bottom row: the corresponding period diagrams. The scenarios are shown for system (1) at $a=1$, $l=-1$, and $b=-0.3$ (a); $b=0$ (b); $b=0.3$ (c). The scenario (d) occurs in the same system at $b=0.46$, $\mu=-50$, and $l=-1$.

considering several border collision induced codimension-three bifurcations.

II. AN EXAMPLE

To illustrate the problem, let us consider the dynamics of the Σ/Δ modulator commonly used in analog to digital converters, which can be expressed by the map [7] given by

$$x_{n+1} = px_n + s - \mathrm{sgn}(x_n). \tag{2}$$

Here $s \in [-1,1]$ is the input signal of the circuit (considered as a parameter of the model), x represents the output, and $p>0$ is a parameter which describes the nonideality of the circuit. Figure 2 shows the regions of different dynamical behaviors in the $s\times p$ parameter space (hereafter called $\Pi_{\Sigma/\Delta}$), exhibiting transitions from periodicity to chaos as well as a period adding structure. Since the system is piecewise linear, the bifurcations can occur only when an attractor (fixed point or a periodic orbit) collides with the border $x=0$, resulting in the destruction of that attractor. This allows us to calculate the corresponding bifurcation curves analytically, which are shown in the figure.

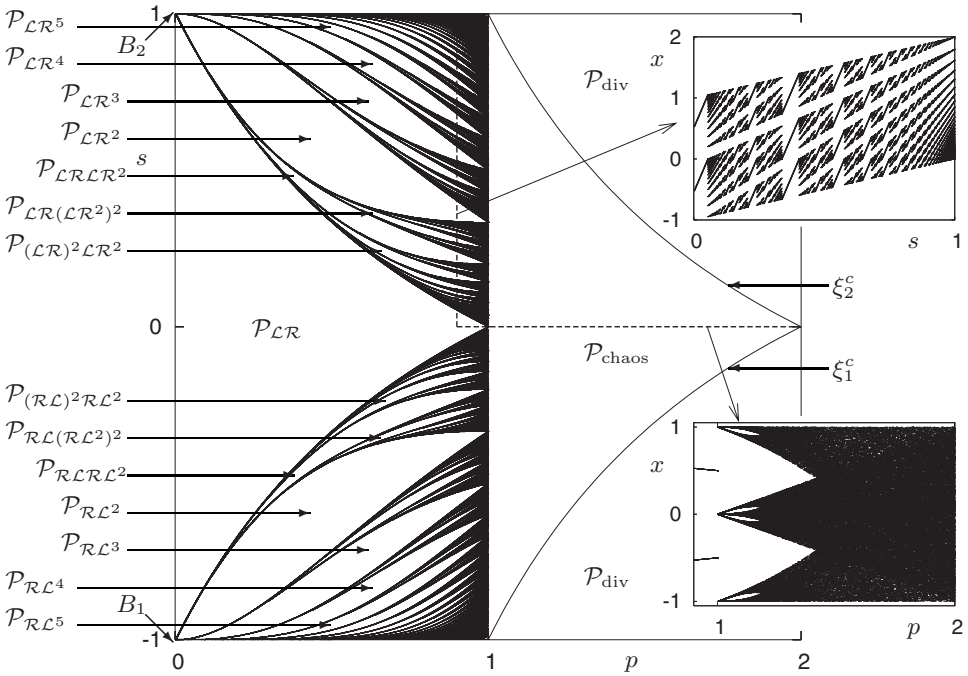

FIG. 2. Numerically calculated bifurcation structures of the Σ/Δ modulator in the parameter plane $\Pi_{\Sigma/\Delta}$ caused by border collision bifurcations. Marked are areas corresponding to periodic dynamics with different periods as well as chaotic and divergent behavior. The numerically calculated insets show the bifurcation diagrams along the marked lines.

In the following discussion, we denote a point $x<0$ by the symbol $\mathcal{L}$, a point $x>0$ by the symbol $\mathcal{R}$, a periodic orbit corresponding to symbolic sequence σ as O_σ, and its region of stability in the parameter space as $\mathcal{P}_\sigma$. Note, that two areas $\mathcal{P}_\sigma$ and $\mathcal{P}_\varrho$ may overlap, leading to a coexistence of attractors.

In the left-hand part of Fig. 2 we observe a large area $\mathcal{P}_{\mathcal{LR}}$ of period-2 behavior. Below and above this area an infinite number of bifurcation curves is located, originating from the points $B_1=(0,-1)$ and $B_2=(0,1)$. Thus, B_1 and B_2 represent codimension-two big bang bifurcation points which organize the complete structure of the parameter plane $\Pi_{\Sigma/\Delta}$ for $p<1$. The bifurcation curves originating at B_1 and B_2 bound the existence areas of stable orbits corresponding to symbolic sequences σ, where σ may be a basic sequence $\mathcal{LR}^n$, $\mathcal{RL}^n$ or composite sequences like $\mathcal{LR}^n\mathcal{LR}^{n+1}$or $\mathcal{RL}^n\mathcal{RL}^{n+1}$. This scenario is governed by the infinite sequence adding scheme, so that between the areas $\mathcal{P}_\sigma$ and $\mathcal{P}_\rho$ there is the area $\mathcal{P}_{\sigma\rho}$ as discussed in Sec. I.

Varying the parameter s across the border collision bifurcation curves as shown in the top inset of Fig. 2, we observe the period adding scenario. Since the adding process continues *ad infinitum*, this scenario includes attractors with arbitrary high periods and as a limiting case aperiodic attractors. These attractors are not chaotic in the sense that they have negative Lyapunov exponents. Owing to the identical slopes of the system function on both sides of the discontinuity point $x=0$, the Lyapunov exponent is given by $\ln(p)$ for any attractor of system (2). It is an inherent property of the period adding scenario, that the size of the parameter area leading to a specific period decreases towards zero with periods increasing to infinity. As a consequence, the existence areas of aperiodic attractors are given by curves in the 2D parameter space, so that these attractors are not robust.

The area of stable periodic and aperiodic nonchaotic dynamics mentioned above is bounded by the line where the Lyapunov exponent is zero, i.e., by the condition $p=1$. Beyond this line, the asymptotic dynamics of system (2) is chaotic and after that divergent [see areas $\mathcal{P}_{\text{chaos}}$ and $\mathcal{P}_{\text{div}}$ in Fig. 2, separated from each other by the curves of boundary crises $\xi_{1,2}^c=\mp(p-2)/p$]. The transition to chaos under variation of the parameter p is illustrated by the bottom inset. In this paper we seek to explain how such bifurcation structures are organized.

Using the substitution $x\to x/2$, $a\to p$, $b\to p$, $\mu\to(s+1)/2$, it can be shown that system (2) represents a special case of the more general model (1). Thus, the structure of the parameter plane $\Pi_{\Sigma/\Delta}$ of system (2) can be explained considering system (1) for $l=-1$.

III. THE STRUCTURE OF THE PARAMETER SPACE OF SYSTEM (1)

We now turn our attention to the more general model (1) in order to explore the underlying mechanism that creates the bifurcation structures shown in Fig. 1, and observed in many physical systems.

An inherent property of system (1), which is reflected in the structures of its parameter space, is given by the symmetry

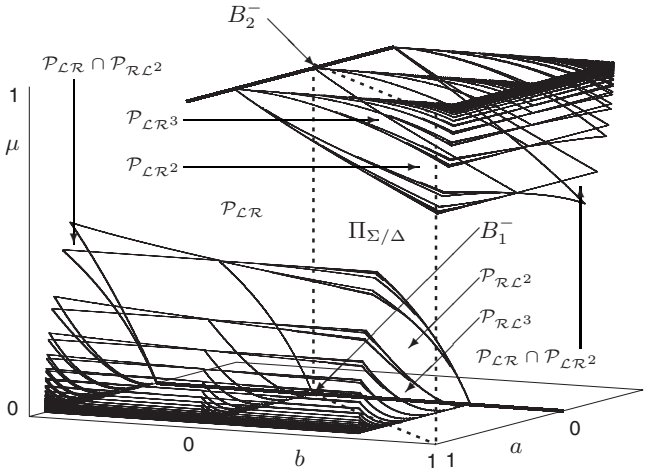

FIG. 3. Numerically determined bifurcation structures formed by codimension-one border collision bifurcation surfaces of system (1) for the case $l=-1$ induced by the two codimension-three big bang bifurcations at the points $B_1^-=(0,0,0)$ and $B_2^-=(0,0,1)$. The dashed lines mark the plane $\Pi_{\Sigma/\Delta}$ to demonstrate the connection to Fig. 2.

$$f(x,a,b,\mu,l)=-f[-x,b,a,-(\mu+l),l]. \tag{3}$$

This symmetry implies that the BBBs described below occur pairwise and produce identical structures in the parts of the parameter space, which can be mapped onto each other by Eq. (3). Due to the replacement of x by $-x$, the involved symbolic sequences are inverted as well. Note also that the parameters in (1) can be scaled so that the length of the discontinuity takes the value -1, 0, or $+1$. These three values of l therefore suffice in the exploration of the generic bifurcation patterns in this system.

A. The case of negative discontinuity

The numerically determined bifurcation structures in the $a\times b\times\mu$ parameter space of system (1) for the case $l=-1$ are presented in Fig. 3. It shows that two codimension-three big bang bifurcations at the points $B_1^-=(0,0,0)$ and $B_2^-=(0,0,1)$ determine the dynamics of system (1) in large parts of the parameter space [8].

These codimension-three big bang bifurcations are caused by the intersection of an infinite number of codimension-two big bang bifurcation curves, which are themselves caused by the intersection of an infinite number of codimension-one border collision bifurcation surfaces as presented in detail in [3]. The stable periodic orbits undergoing these border collision bifurcations are, like in the case of system (2), the orbits corresponding to the basic sequences $\mathcal{LR}^n$, $\mathcal{RL}^n$ or composite sequence derived from them.

Note, that in the notation $B_{1,2}^-$ we use here, the superscript $-$ refers to the case of negative discontinuity, i.e., $l=-1$. Note further, that not only the stable periodic orbits corresponding to finite symbolic sequences and the stable aperiodic orbits corresponding to infinite symbolic sequences but also unstable periodic orbits and even chaotic attractors are influenced or organized by the character of these two codimension-three bifurcations.

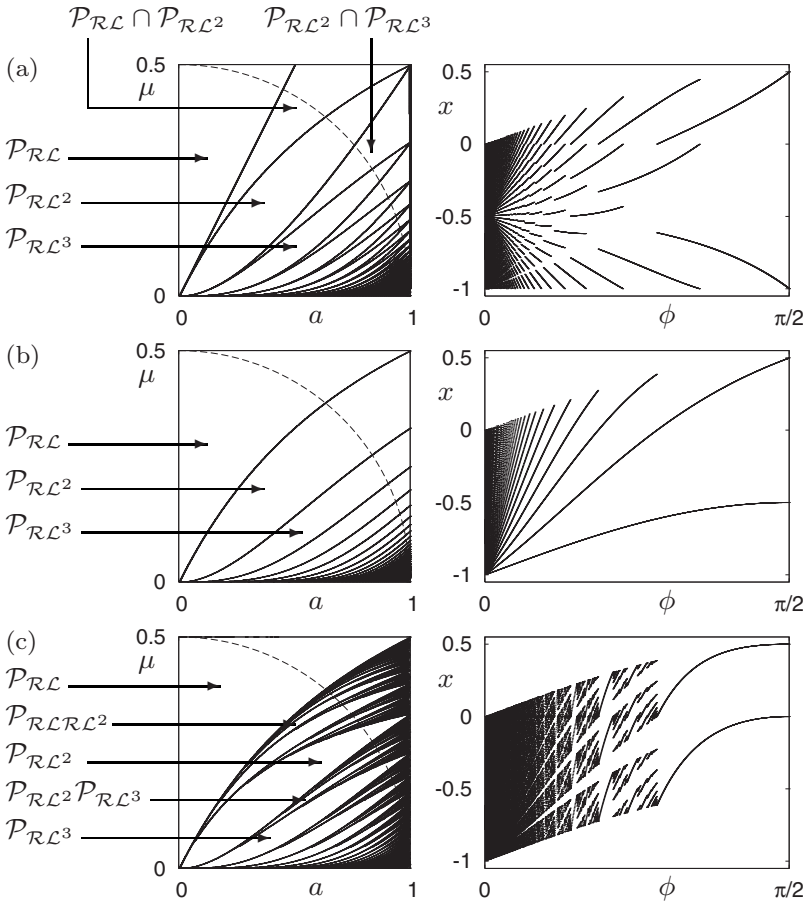

FIG. 4. Left: two-parameter bifurcation diagrams showing numerically determined unfoldings of the three types of codimension-two big bang bifurcations, generating (a) a period increment scenario with pairwise coexistence of periodic orbits for $b=-1$, (b) a pure period increment scenario for $b=0$, and (c) a period adding scenario for $b=1$. Right: bifurcation scenarios along the arc around the codimension-two bifurcation points marked in each figure in the left-hand column.

We define the *influence region* of a bifurcation point as the contiguous region around it, where the parameter setting leads to attractors which are topologically equivalent to the attractors existing in the vicinity of the bifurcation point. In Fig. 3, in the left-hand part of the influence region of B_1^- the period increment scenario with pairwise coexistence of attractors takes place [as illustrated in Fig. 4(a)], whereas in the middle part the pure period increment scenario takes place [see Fig. 4(b)] and in the right-hand part the period adding scenario occurs [compare Fig. 4(c)]. Owing to the symmetry of the parameter space, in the rear part of the influence region of B_2^- the period increment scenario with pairwise coexistence of attractors exists, in the middle part the pure period increment scenario, and in the front part the period adding scenario occurs.

The influence regions of B_1^- and B_2^- are separated from each other by the area $\mathcal{P}_{\mathcal{LR}}$, which has a complex 3D shape and overlaps with the area $\mathcal{P}_{\mathcal{RL}^2}$ in the left-hand part of the figure and with the area $\mathcal{P}_{\mathcal{LR}^2}$ in the rear part. Note that although the areas $\mathcal{P}_{\mathcal{LR}^n}$, $\mathcal{P}_{\mathcal{RL}^n}$ are now 3D, the bounding border collision bifurcation surfaces can still be calculated analytically.

Based on these observations, we claim that the complete bifurcation structure rests on the two codimension-three BBB points occurring at $B_1^-=(0,0,0)$ and $B_2^-=(0,0,1)$. Because both codimension-three bifurcations are of the same type, we will describe only one of them in detail, namely the one occurring at B_1^-. In order to do that, we consider three parameter planes for fixed values of b in the characteristic cases $b<0$, $b=0$, and $b>0$.

Case $b<0$. In the $a\times\mu$ planes one observes period increment bifurcation structures with coexistence of attractors illustrated in Fig. 4(a). Consequently, the bifurcation point at the origin of each plane is a period increment BBB with coexistence of attractors.

Case $b=0$. In the $a\times\mu$ plane one observes a pure period increment bifurcation structure [see Fig. 4(b)]. The bifurcation point at the origin is a pure period increment big bang bifurcation.

Case $b>0$. In the $a\times\mu$ planes one observes period adding structures [see Fig. 4(c)]. Consequently, the bifurcation point at the origin of each plane is a period adding big bang bifurcation. In this case parameter values leading to attractors of increasingly high periodicities accumulate towards specific curves in the parameter space, corresponding to nonrobust aperiodic nonchaotic attractors as described earlier.

Note, that the plane $b=0$ separates the period increment structures from the period adding structures. Figure 3 also shows that in this plane the separating lines between regions with two subsequent periods are all codimension-two lines, i.e., every point on these lines correspond to a codimension-two bifurcation. Therefore, this plane is denoted as the 2D characteristic manifold of the described type of codimension-three bifurcation. Additionally, the line $a=0$, $\mu=0$ is a line of codimension-two bifurcations as well. For values $b<0$ each point on this line represents a period increment BBB with coexistence of attractors, for $b=0$ it represents a pure period increment BBB, and finally for $b>0$ each point on this line represents a period adding BBB. Since each of these bifurcations is a codimension-two bifurcation, and at the point B_1^-

the type of the codimension-two bifurcation changes, this point represents a codimension-three bifurcation point. In the following, the line $a=0$, $\mu=0$ is denoted as the 1D characteristic manifold of the described type of codimension-three bifurcation. Similar results can be obtained for the second codimension-three period adding BBB occurring at the point B_2^-. To this point, the following objects form the skeleton of the bifurcation structure in the 3D parameter space.

Bifurcation point	2D manifold	1D manifold
$B_1^-=(0,0,0)$	$\subset(b=0)$	$a=0$, $\mu=0$
$B_2^-=(0,0,1)$	$\subset(a=0)$	$b=0$, $\mu=1$

Note that when dealing with specific piecewise smooth maps, it is necessary to determine these two characteristic manifolds, because they represent the skeleton of the complete 3D bifurcation structure.

B. The case of positive discontinuity

Next we investigate system (1) for the case $l=+1$. As shown in [6], the structure of the 3D parameter space in this case is determined by the following four codimension-three BBBs of the same type as described above:

Bifurcation point	2D manifold	1D manifold
$B_1^+=(0,-1,0)$	$\subset(a=0)$	$b=-1$, $\mu=0$
$B_2^+=(0,-1,\infty)$	$\subset(a=0)$	$b=-1$, $\mu=\infty$
$B_3^+=(-1,0,-1)$	$\subset(b=0)$	$a=-1$, $\mu=-1$
$B_4^+=(-1,0,-\infty)$	$\subset(b=0)$	$a=-1$, $\mu=-\infty$

Note that the BBBs B_2^+ and B_4^+ occur at infinite parameter values. Nevertheless, it is not only of theoretical interest to investigate these bifurcations, because a codimension-three bifurcation typically possesses an extended influence region. Even in the case where the bifurcation itself occurs at infinity, the influence region reaches finite parameter values. The structure emerging at this bifurcation point located at infinity determines the behavior in the domains of finite and practically interesting parameter values. Hence, in order to make the overall structure of the parameter space visualizable, we apply the coordinate transformation $\eta\rightarrow\arctan(\eta)$ for $\eta\in\{a,b,\mu\}$. The resulting structure of the parameter space is shown in Fig. 5. The character of the bifurcation sequences induced by $B_{1,2,3,4}^+$ is similar to those observed for the case of negative discontinuity, i.e., those shown in Fig. 4.

In the case $l=1$, the 1D characteristic manifolds of the big bang bifurcations B_1^+ and B_2^+ are parallel to each other and their 2D characteristic manifolds lie in the same plane, as shown in Fig. 5. Due to the symmetry (3), the structure induced by the BBBs B_3^+ and B_4^+, is identical with the structure described above.

C. The case of continuous map

For $l=0$, system (1) is a continuous map for which some results are presented in [9]. In this case codimension-three

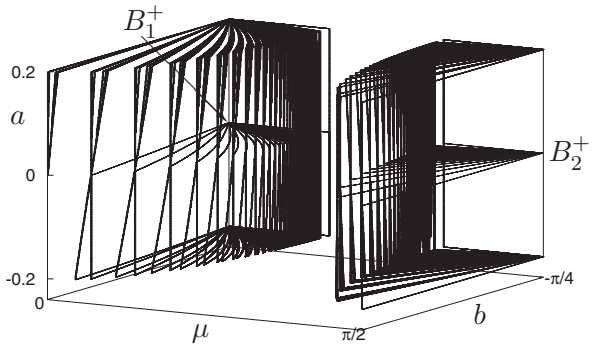

FIG. 5. Numerically determined bifurcation structures formed by codimension-one border collision bifurcation surfaces of system (1) for the case $l=1$ induced by the two codimension-three big bang bifurcations at the points $B_1^+=(0,-1,0)$ and $B_2^+=(0,-1,\infty)$. Note that the coordinate transformation $\eta\rightarrow\arctan(\eta)$ for $\eta\in\{a,b,\mu\}$ has been used to locate the codimension-three bifurcation point within finite parameter range. B_3^+ and B_4^+ are not shown for the sake of clarity of the diagram, but their existence can be inferred because of the symmetry of the parameter space.

bifurcations of the type described above do not occur. Instead, the 3D parameter space is organized by the following four codimension-three bifurcations which are of a different type:

Bifurcation point	2D manifold	1D manifold
$B_1^{-0+}=(0,-\infty,\infty)$	$\subset(\mu=\infty)$	$a=0$, $b=-\infty$
$B_2^{-0+}=(-\infty,0,-\infty)$	$\subset(\mu=-\infty)$	$a=-\infty$, $b=0$
$B_1^0=(0,-\infty,0)$	$\subset(\mu=0)$	$a=0$, $b=-\infty$
$B_2^0=(-\infty,0,0)$	$\subset(\mu=0)$	$a=-\infty$, $b=0$

Concerning the notation of these bifurcation points, recall that the superscript is related to the values of the parameter l, for which the corresponding bifurcations occur. Therefore, the notation $B_{1,2}^{-0+}$ means that these bifurcations exist in all three cases $l<0$, $l=0$, and $l>0$, whereas the bifurcations $B_{1,2}^0$ occur only in the case $l=0$ [10].

Because the structures induced by all four bifurcations are identical, let us investigate the point B_1^0 in detail. Figure 6(b) represents a typical bifurcation scenario, reported for many practical applications [11,12]. It shows a sequence of periodic dynamics with increasing periods and chaotic windows between the consecutive periodic windows. This scenario can be explained from the structure of the plane $a\times b$ for a positive value of μ shown in Fig. 6(a). In this plane each region $\mathcal{P}_{\mathcal{LR}^n}$ is bounded by two curves: $\xi_{\mathcal{LR}^n}$ corresponding to the birth of the periodic orbit $O_{\mathcal{LR}^n}$, and $\theta_{\mathcal{LR}^n}$ corresponding to it becoming unstable. For each n both curves originate from the point $(0,-\infty)$, so that this point represents a codimension-two big bang bifurcation. Because the structure of the 3D parameter space is the same for all positive values of μ, the point B_1^0 represents a codimension-three bifurcation. This is clearly visible in Fig. 6(c) where the structure of the 3D parameter space is presented. The cuboid in the middle part represents the stability area $\mathcal{P}_{\mathcal{R}}$ of the fixed point $x_{\mathcal{R}}=\mu/(1-b)$, whereas the prismlike structure in the front

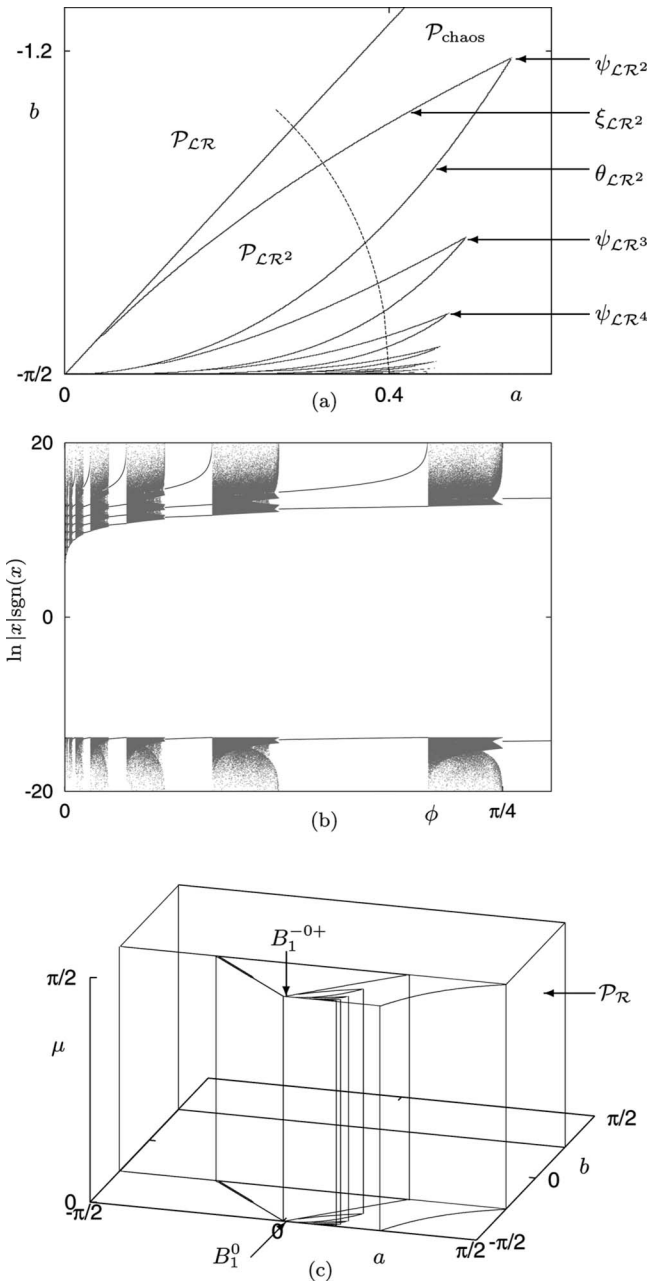

FIG. 6. (a) Analytically determined structure of the plane $a \times b$ in the region of periodic and chaotic dynamics for $l=0$ and a sufficiently large value of μ. (b) Bifurcation scenario along the arc marked in (a) calculated numerically. (c) Analytically calculated structure of the 3D parameter space $a \times b \times \mu$ in the case $l=0$ for $\mu > 0$. Note that the same parameter scaling as in Fig. 5 is used here.

represents the stability area $\mathcal{P}_{\mathcal{LR}}$ of the period-2 solution corresponding to the symbolic sequence $\mathcal{LR}$. The adjacent 3D region to the right of the prism and to the front of the cuboid, represents the influence regions of the codimension-three bifurcations B_1^0 and B_1^{-0+}. In this region, the stable periodic solutions with symbolic sequences $\mathcal{LR}^n$ take place, whereby between two regions corresponding to successive sequences $\mathcal{LR}^n$ and $\mathcal{LR}^{n+1}$ a region with chaotic dynamics is located as shown in more detail in Fig. 6(a).

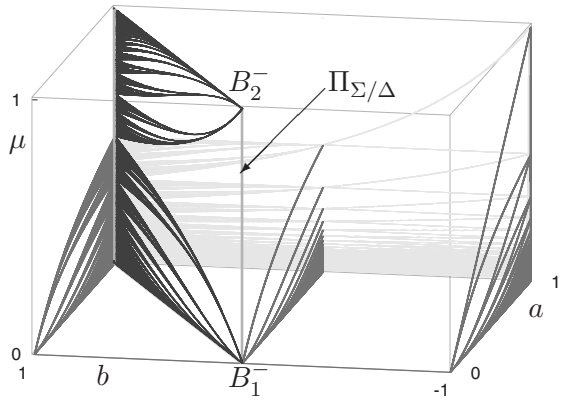

FIG. 7. Bifurcation structures corresponding to the influence region of the codimension-three bifurcation B_1^- and an embedding of the plane $\Pi_{\Sigma/\Delta}$ in this structure.

Let us consider additionally the points $\psi_{\mathcal{LR}^n}$, where the curves $\xi_{\mathcal{LR}^n}$ and $\theta_{\mathcal{LR}^n}$ intersect [see Fig. 6(a)]. It can be shown that for increasing n the sequence of these points converges monotonously to the point $(1/2, -\infty)$. Hence, if the parameters are varied along an arc with a fixed radius $R > 1/2$ around the point B_1^0, the observed bifurcation sequence [similar to the one shown in Fig. 6(b)] becomes truncated. For any radius $R > 1/2$ there exists a number m for which the distance between the points $\psi_{\mathcal{LR}^m}$ and B_1^0 is less than R. Therefore, in the above-mentioned bifurcation scenario only periodic orbits $O_{\mathcal{LR}^n}$ with $n < m$ are involved. In contrast to this, for $R \leqq 1/2$ this scenario takes place *ad infinitum*.

Remarkably, the structure induced by the codimension-three BBB occurring at the point B_1^{-0+} is identical with the structure induced by the codimension-three BBB B_1^0 described above. This is based on the fact that in the case $l=0$, a suitable scaling allows to reduce system (1) to the three cases $\mu < 0$, $\mu = 0$, and $\mu > 0$. It is clearly visible in Fig. 6(c), that the structure of the parameter space does not depend on the parameter μ in the complete interval $(0, \infty)$. Since the structures induced by B_1^0 and B_1^{-0+} belong both to the parameter interval $\mu \in (0, \infty)$, the both BBBs must be of the same type. Note, that the BBBs occurring at the points B_2^0 and B_2^{-0+}, are equivalent to B_1^0 and B_1^{-0+}as a consequence of the symmetry (3).

Next, let us consider what happens with the topological structure of the 3D parameter space of system (1) under variation of the parameter l. For $l \in (-\infty, 0)$ and for $l \in (0, \infty)$ this structure does not change. In contrast, varying l from negative to positive values, one observes that the codimension-three bifurcations $B_{1,2}^-$ are destroyed and $B_{1,2,3,4}^+$ emerge. Hence, the bifurcation occurring at $l=0$ is a *codimension-four bifurcation*. This bifurcation requires a more detailed investigation, which remains for future work.

IV. APPLICATION TO THE Σ/Δ MODULATOR

With this framework, the bifurcation structure of system (2) can now be explained easily. The parameter plane $p \times s$ shown in Fig. 2 corresponds in the case of system (1) to the

case $l=-1$, and the diagonal plane $(a=b)\times\mu$. Because $p>0$ and $s\in[-1,1]$, only this region of the plane is relevant for us, which is marked in Fig. 3 as $\Pi_{\Sigma/\Delta}$. As one can see, both codimension-three BBBs occurring at the points $B^{-}_{1,2}$ in the $a\times b\times\mu$ space belong to $\Pi_{\Sigma/\Delta}$ and correspond to the points $B_{1,2}$ in the original system. Remarkably, $\Pi_{\Sigma/\Delta}$ intersects only the adding part of the influence regions of $B^{-}_{1,2}$, whereas the increment part of these influence regions is not intersected by $\Pi_{\Sigma/\Delta}$. This explains why we observe the period adding structures shown in Fig. 2 and not the period increment structures. This is illustrated in Fig. 7, where an embedding of the plane $\Pi_{\Sigma/\Delta}$ in the influence region of the point B^{-}_{1} is shown. As one can see, the lower part of the bifurcation structure of the plane $\Pi_{\Sigma/\Delta}$ is induced by B^{-}_{1}, whereas the upper one is induced by B^{-}_{2}. For the sake of clarity, only the intersection of the plane $\Pi_{\Sigma/\Delta}$ with the structure induced by B^{-}_{1} is shown in Fig. 7.

Note, that the structure of the area $\mathcal{P}_{\text{chaos}}$ with chaotic dynamics shown in Fig. 2 is also influenced by $B_{1,2}$ (respectively, by $B^{-}_{1,2}$). This is because the chaotic attractors are organized by unstable periodic orbits, which emerge at these bifurcations and become unstable at the boundary of their influence regions. However, it is beyond the scope of this paper to discuss this topic in detail.

V. CONCLUSIONS

We thus conclude that the complex bifurcation sequences observed in nonsmooth systems can be understood in terms of only a few codimension-three big bang bifurcations, and their respective characters and influence regions in the parameter space. When applying this concept to any physical system exhibiting period-increment and period-adding cascades, one must identify these codimension-three big bang bifurcation points, and their 1D and 2D manifolds. These form a skeleton in the parameter space on which the overall bifurcation structure of the system rests. We have demonstrated how this idea can be applied to a practical dynamical system—the Σ/Δ modulator, and which explains the underlying mechanism behind the structure of bifurcation diagrams exhibited by this system.

[1] C. Budd and F. Dux, Philos. Trans. R. Soc. London, Ser. A **347**, 365 (1994); J. Finkeová, M. Dolnik, B. Hrudka, and M. Marek, J. Phys. Chem. **94**, 4110 (1990); P. Tracqui, Acta Biotheor. **42**, 147 (1994). Y.-F. Huang, T.-C. Yen, and J.-L. Chern, Phys. Lett. A **199**, 70 (1995); A. E. Aroudi, L. Benadero, E. Toribio, and G. Olivar, IEEE Trans. Circuits Syst., I: Fundam. Theory Appl. **46**, 1374 (1999); S. Coombes and A. H. Osbaldestin, Phys. Rev. E **62**, 4057 (2000).

[2] H. Bai-lin, *Elementary Symbolic Dynamics and Chaos in Dissipative Systems* (World Scientific, Singapore, 1989).

[3] V. Avrutin and M. Schanz, Nonlinearity **19**, 531 (2006).

[4] O. Feely and L. Chua, Int. J. Bifurcation Chaos Appl. Sci. Eng. **22**, 325 (1992); G. Maggio, M. di Bernardo, and M. Kennedy, IEEE Trans. Circuits Syst., I: Fundam. Theory Appl. **47**, 1160 (2000); S. Banerjee, S. Parui, and A. Gupta, IEEE Trans. Circuits Syst., II: Analog Digital Signal Process. **51**, 649 (2004); A. Sharkovsky and L. Chua, IEEE Trans. Circuits Syst., I: Fundam. Theory Appl. **40**, 722 (1993).

[5] P. Jain and S. Banerjee, Int. J. Bifurcation Chaos Appl. Sci. Eng. **13**, 3341 (2003); S. Hogan, L. Higham, and T. Griffin, Proc. R. Soc. London, Ser. A **463**, 49 (2007).

[6] V. Avrutin, M. Schanz, and S. Banerjee, Nonlinearity **19**, 1875 (2006).

[7] O. Feely and L. O. Chua, IEEE Trans. Circuits Syst. **38**, 1293 (1991).

[8] Here we confine our attention to the region of the parameter space $a=[-1,1]$, $b=[-1,1]$, $\mu=[0,1]$. There are other codimension-three big bang bifurcation points outside this region, which we do not discuss in this paper in order to avoid the exposition becoming too involved.

[9] H. E. Nusse and J. A. Yorke, Int. J. Bifurcation Chaos Appl. Sci. Eng. **5**, 189 (1995); S. Banerjee, M. S. Karthik, G. H. Yuan, and J. A. Yorke, IEEE Trans. Circuits Syst., I: Fundam. Theory Appl. **47**, 389 (2000).

[10] Note that the points $B^{-0+}_{1,2}$ also exist in the cases of negative and positive discontinuity. For example, in case of negative discontinuity, these bifurcations occur at the boundary of the influence regions of $B^{-}_{1,2}$ in the increment part, which was outside the region of the parameter space considered in Fig. 3.

[11] J. M. Perez, Phys. Rev. A **32**, 2513 (1985);

[12] P. Piiroinen, L. Virgin, and A. Champneys, J. Nonlinear Sci. **14**, 383 (2004).